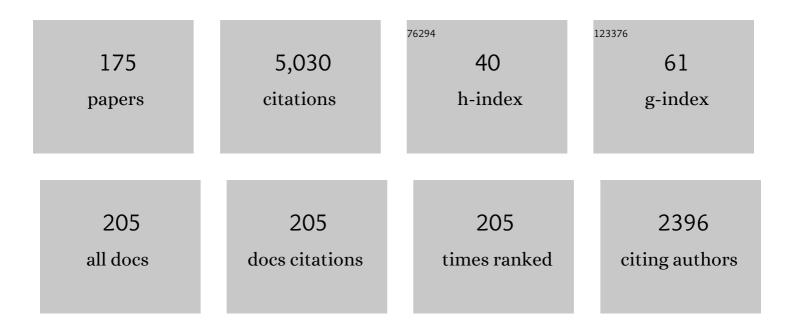
Shuangfang Lu

List of Publications by Year in descending order

Source: https://exaly.com/author-pdf/2757898/publications.pdf Version: 2024-02-01



#	Article	IF	CITATIONS
1	Pore size distributions contributed by various components in the Upper Ordovician Wufeng Shale from Southeast Chongqing, China. Journal of Petroleum Science and Engineering, 2022, 208, 109230.	2.1	4
2	Mechanism and geological significance of anomalous negative δ13Ckerogen in the Lower Cambrian, NW Tarim Basin, China. Journal of Petroleum Science and Engineering, 2022, 208, 109384.	2.1	22
3	Insights into the pore structure and pore development pattern of subaqueous volcanic rocks in the Santanghu Basin, western China. Marine and Petroleum Geology, 2022, 135, 105387.	1.5	6
4	The upper and lower limits and grading evaluation of the Shahezi tight gas reservoirs in the Xujiaweizi Rift, northern Songliao Basin: Implications from microscopic pore structures. Journal of Petroleum Science and Engineering, 2022, 212, 110224.	2.1	5
5	Evaluating microdistribution of adsorbed and free oil in a lacustrine shale using nuclear magnetic resonance: A theoretical and experimental study. Journal of Petroleum Science and Engineering, 2022, 212, 110208.	2.1	18
6	NMR characterization of fluid mobility in low-permeability conglomerates: An experimental investigation of spontaneous imbibition and flooding. Journal of Petroleum Science and Engineering, 2022, 214, 110483.	2.1	7
7	Multi-scale pore structure characterization of lacustrine shale and its coupling relationship with material composition: An integrated study of multiple experiments. Marine and Petroleum Geology, 2022, 140, 105648.	1.5	30
8	Novel Self-Adaptive Shale Gas Production Proxy Model and Its Practical Application. ACS Omega, 2022, 7, 8294-8305.	1.6	5
9	Research Progress of Microscopic Pore–Throat Classification and Grading Evaluation of Shale Reservoirs: A Minireview. Energy & Fuels, 2022, 36, 4677-4690.	2.5	6
10	Pore Structure and Multifractal Characteristics of Overmature Continental Shale: A Case Study from the Xujiaweizi Fault Depression, Songliao Basin, China. Geofluids, 2022, 2022, 1-13.	0.3	4
11	Key Oil Content Parameter Correction of Shale Oil Resources: A Case Study of the Paleogene Funing Formation, Subei Basin, China. Energy & Fuels, 2022, 36, 5316-5326.	2.5	8
12	Determination of in situ hydrocarbon contents in shale oil plays. Part 1: Is routine Rock–Eval analysis reliable for quantifying the hydrocarbon contents of preserved shale cores?. Organic Geochemistry, 2022, 170, 104449.	0.9	12
13	Unsupervised contrastive learning for few-shot TOC prediction and application. International Journal of Coal Geology, 2022, 259, 104046.	1.9	6
14	The Gas Content Characteristics of Nanopores Developed in a Normal Pressure Shale Gas Reservoir in Southeast Chongqing, Sichuan Basin, China. Journal of Nanoscience and Nanotechnology, 2021, 21, 698-706.	0.9	0
15	Simulation of Oil-Water Rock Wettability of Different Constituent Alkanes on Kaolinite Surfaces at the Nanometer Scale. Journal of Nanoscience and Nanotechnology, 2021, 21, 225-233.	0.9	2
16	Comparison of Marine and Continental Shale Gas Reservoirs and Their Gas-Bearing Properties in China: The Examples of the Longmaxi and Shahezi Shales. Energy & Fuels, 2021, 35, 4029-4043.	2.5	13
17	Analysis of Adsorption Characteristics and Influencing Factors of Wufeng–Longmaxi Formation Shale in Sichuan Basin. Energy & Fuels, 2021, 35, 4925-4942.	2.5	13
18	Critical factors controlling adsorption capacity of shale gas in Wufeng-Longmaxi formation, Sichuan Basin: Evidences from both experiments and molecular simulations. Journal of Natural Gas Science and Engineering, 2021, 88, 103774.	2.1	24

#	Article	IF	CITATIONS
19	Geochemical modeling of carbon isotope fractionation during methane transport in tight sedimentary rocks. Chemical Geology, 2021, 566, 120033.	1.4	32
20	Classification Evaluation of Gas Shales Based on High-Pressure Mercury Injection: A Case Study on Wufeng and Longmaxi Formations in Southeast Sichuan, China. Energy & Fuels, 2021, 35, 9382-9395.	2.5	9
21	Impacts of gas pressure on carbon isotope fractionation during methane degassing—An experimental study on shales from Wufeng and Longmaxi Formations in southeast Sichuan, China. Marine and Petroleum Geology, 2021, 128, 105001.	1.5	14
22	Pore Structure and Fractal Character of Lacustrine Oil-Bearing Shale from the Dongying Sag, Bohai Bay Basin, China. Geofluids, 2021, 2021, 1-19.	0.3	4
23	A Novel Shale Gas Production Prediction Model Based on Machine Learning and Its Application in Optimization of Multistage Fractured Horizontal Wells. Frontiers in Earth Science, 2021, 9, .	0.8	5
24	Classification and control factors of pore-throat systems in hybrid sedimentary rocks of Jimusar Sag, Junggar Basin, NW China. Petroleum Exploration and Development, 2021, 48, 835-849.	3.0	11
25	Influence of a Paleosedimentary Environment on Shale Oil Enrichment: A Case Study on the Shahejie Formation of Raoyang Sag, Bohai Bay Basin, China. Frontiers in Earth Science, 2021, 9, .	0.8	8
26	Characteristics of Shale Wettability by Contact Angle and Its Influencing Factors: A Case Study in Songliao. Frontiers in Earth Science, 2021, 9, .	0.8	8
27	Improved Methane Adsorption Model in Shale by Considering Variable Adsorbed Phase Density. Energy & Fuels, 2021, 35, 2064-2074.	2.5	12
28	Wettability and Its Controlling Factors of Mixed Shale Oil Reservoirs: A Case Study of Permian Lucaogou Formation in Jimusar Sag. Lithosphere, 2021, 2021, .	0.6	2
29	Limits and grading evaluation criteria of tight oil reservoirs in typical continental basins of China. Petroleum Exploration and Development, 2021, 48, 1089-1100.	3.0	26
30	Estimation of gas-in-place content in coal and shale reservoirs: A process analysis method and its preliminary application. Fuel, 2020, 259, 116266.	3.4	61
31	A new method for predicting sweet spots of shale oil using conventional well logs. Marine and Petroleum Geology, 2020, 113, 104097.	1.5	21
32	Classification of the tight oil reservoir storage space in the Raoyang Sag of the Jizhong Depression in the Bohai Bay Basin, China. Energy Science and Engineering, 2020, 8, 74-88.	1.9	6
33	Geochemical characteristics and effectiveness of thick, black shales in southwestern depression, Tarim Basin. Journal of Petroleum Science and Engineering, 2020, 185, 106607.	2.1	17
34	Applicability of fractal capillary pressure models to sandstones. Journal of Petroleum Science and Engineering, 2020, 185, 106626.	2.1	12
35	Broad ion beam-scanning electron microscopy pore microstructure and multifractal characterization of shale oil reservoir: A case sample from Dongying Sag, Bohai Bay Basin, China. Energy Exploration and Exploitation, 2020, 38, 613-628.	1.1	21
36	1D and 2D Nuclear magnetic resonance (NMR) relaxation behaviors of protons in clay, kerogen and oil-bearing shale rocks. Marine and Petroleum Geology, 2020, 114, 104210.	1.5	89

#	Article	IF	CITATIONS
37	Key factors influencing the low-field NMR characterisation of gas- and oil-bearing shales: a case study of the shales from the southern Sichuan Basin and Dongying sag, China. International Journal of Oil, Gas and Coal Technology, 2020, 24, 466.	0.1	2
38	Application of the combination of high-pressure mercury injection and nuclear magnetic resonance to the classification and evaluation of tight sandstone reservoirs: A case study of the Linxing Block in the Ordos Basin. Natural Gas Industry B, 2020, 7, 433-442.	1.4	19
39	Pore size distributions contributed by OM, clay and other minerals in over-mature marine shale: A case study of the Longmaxi shale from Southeast Chongqing, China. Marine and Petroleum Geology, 2020, 122, 104679.	1.5	28
40	Pore development of the Lower Longmaxi shale in the southeastern Sichuan Basin and its adjacent areas: Insights from lithofacies identification and organic matter. Marine and Petroleum Geology, 2020, 122, 104662.	1.5	24
41	Controls on Pore Structures and Permeability of Tight Gas Reservoirs in the Xujiaweizi Rift, Northern Songliao Basin. Energies, 2020, 13, 5184.	1.6	3
42	Carbon isotope fractionation during shale gas transport: Mechanism, characterization and significance. Science China Earth Sciences, 2020, 63, 674-689.	2.3	34
43	Quantifying the control of pore types on fluid mobility in low-permeability conglomerates by integrating various experiments. Fuel, 2020, 275, 117835.	3.4	14
44	Adsorbed and free hydrocarbons in unconventional shale reservoir: A new insight from NMR T1-T2 maps. Marine and Petroleum Geology, 2020, 116, 104311.	1.5	72
45	Paleoweathering, hydrothermal activity and organic matter enrichment during the formation of earliest Cambrian black strata in the northwest Tarim Basin, China. Journal of Petroleum Science and Engineering, 2020, 189, 106987.	2.1	39
46	Oil charging model and controlling factors revealed by an online nuclear magnetic resonance (NMR) system. Marine and Petroleum Geology, 2020, 118, 104442.	1.5	8
47	Characterization of Shale Pore Size Distribution by NMR Considering the Influence of Shale Skeleton Signals. Energy & Fuels, 2019, 33, 6361-6372.	2.5	22
48	Study on the Full-Range Pore Size Distribution and the Movable Oil Distribution in Glutenite. Energy & Fuels, 2019, 33, 7028-7042.	2.5	36
49	Climate-Driven Variations in the Depositional Environment and Organic Matter Accumulation of Lacustrine Mudstones: Evidence from Organic and Inorganic Geochemistry in the Biyang Depression, Nanxiang Basin, China. Energy & Fuels, 2019, 33, 6946-6960.	2.5	13
50	A novel approach to the quantitative evaluation of the mineral composition, porosity, and kerogen content of shale using conventional logs: A case study of the Damintun Sag in the Bohai Bay Basin, China. Interpretation, 2019, 7, T83-T95.	0.5	3
51	Occurrence mechanism of lacustrine shale oil in the Paleogene Shahejie Formation of Jiyang Depression, Bohai Bay Basin, China. Petroleum Exploration and Development, 2019, 46, 833-846.	3.0	94
52	Evaluation of the total organic carbon of source rocks in lacustrine basins using the variable-coefficient ΔLgR technique — A case study of the Xujiaweizi Fault Depression in the Songliao Basin. Interpretation, 2019, 7, SJ67-SJ75.	0.5	3
53	Pore-Scale CO ₂ Displacement Simulation Based on the Three Fluid Phase Lattice Boltzmann Method. Energy & Fuels, 2019, 33, 10039-10055.	2.5	19
54	Microdistribution and mobility of water in gas shale: A theoretical and experimental study. Marine and Petroleum Geology, 2019, 102, 496-507.	1.5	76

#	Article	IF	CITATIONS
55	A new method for measuring shale porosity with low-field nuclear magnetic resonance considering non-fluid signals. Marine and Petroleum Geology, 2019, 102, 535-543.	1.5	44
56	Total Porosity Measured for Shale Gas Reservoir Samples: A Case from the Lower Silurian Longmaxi Formation in Southeast Chongqing, China. Minerals (Basel, Switzerland), 2019, 9, 5.	0.8	13
57	Investigation of pore size effects on adsorption behavior of shale gas. Marine and Petroleum Geology, 2019, 109, 1-8.	1.5	45
58	Porosity Enhancement Potential through Dolomite Mineral Dissolution in the Shale Reservoir: A Case Study of an Argillaceous Dolomite Reservoir in the Jianghan Basin. Energy & Fuels, 2019, 33, 4857-4864.	2.5	10
59	Facies and the Architecture of Estuarine Tidal Bar in the Lower Cretaceous Mcmurray Formation, Central Athabasca Oil Sands, Alberta, Canada. Energies, 2019, 12, 1769.	1.6	15
60	Pyrolytic Gaseous Hydrocarbon Generation and the Kinetics of Carbon Isotope Fractionation in Representative Model Compounds With Different Chemical Structures. Geochemistry, Geophysics, Geosystems, 2019, 20, 1773-1793.	1.0	7
61	Exploration progress and geochemical features of lacustrine shale oils in China. Journal of Petroleum Science and Engineering, 2019, 178, 975-986.	2.1	77
62	Dynamic Gas Flow in Coals and Its Evaluation. , 2019, , 277-300.		2
63	Effect of sedimentary environment on the formation of organic-rich marine shale: Insights from major/trace elements and shale composition. International Journal of Coal Geology, 2019, 204, 34-50.	1.9	72
64	Evaluation of the density and thickness of adsorbed methane in differently sized pores contributed by various components in a shale gas reservoir: A case study of the Longmaxi Shale in Southeast Chongqing, China. Chemical Engineering Journal, 2019, 367, 123-138.	6.6	24
65	Upscaling of Dynamic Capillary Pressure of Twoâ€Phase Flow in Sandstone. Water Resources Research, 2019, 55, 426-443.	1.7	13
66	Characterization of pore size distributions of shale oil reservoirs: A case study from Dongying sag, Bohai Bay basin, China. Marine and Petroleum Geology, 2019, 100, 297-308.	1.5	63
67	Scale-Dependent Nature of Porosity and Pore Size Distribution in Lacustrine Shales: An Investigation by BIB-SEM and X-Ray CT Methods. Journal of Earth Science (Wuhan, China), 2019, 30, 823-833.	1.1	21
68	The effects of composition, laminar structure and burial depth on connected pore characteristics in a shale oil reservoir, the Raoyang Sag of the Bohai Bay Basin, China. Marine and Petroleum Geology, 2019, 101, 290-302.	1.5	22
69	Fracture types in the lower Cambrian shale and their effect on shale gas accumulation, Upper Yangtze. Marine and Petroleum Geology, 2019, 99, 282-291.	1.5	38
70	Pore Types and Quantitative Evaluation of Pore Volumes in the Longmaxi Formation Shale of Southeast Chongqing, China. Acta Geologica Sinica, 2018, 92, 342-353.	0.8	27
71	FRACTAL NATURE OF POROSITY IN VOLCANIC TIGHT RESERVOIRS OF THE SANTANGHU BASIN AND ITS RELATIONSHIP TO PORE FORMATION PROCESSES. Fractals, 2018, 26, 1840007.	1.8	11
72	The effect of a microscale fracture on dynamic capillary pressure of two-phase flow in porous media. Advances in Water Resources, 2018, 113, 272-284.	1.7	34

#	Article	IF	CITATIONS
73	Factors Affecting Shale Gas Accumulation in Overmature Shales Case Study from Lower Cambrian Shale in Western Sichuan Basin, South China. Energy & Fuels, 2018, 32, 3003-3012.	2.5	30
74	Understanding Model Crude Oil Component Interactions on Kaolinite Silicate and Aluminol Surfaces: Toward Improved Understanding of Shale Oil Recovery. Energy & Fuels, 2018, 32, 1155-1165.	2.5	62
75	Quantitative characterization of organic acid generation, decarboxylation, and dissolution in a shale reservoir and the corresponding applications—A case study of the Bohai Bay Basin. Fuel, 2018, 214, 538-545.	3.4	33
76	GCMC simulations on the adsorption mechanisms of CH4 and CO2 in K-illite and their implications for shale gas exploration and development. Fuel, 2018, 224, 521-528.	3.4	55
77	FRACTAL CHARACTERISTICS OF CONTINENTAL SHALE PORES AND ITS SIGNIFICANCE TO THE OCCURRENCE OF SHALE OIL IN CHINA: A CASE STUDY OF BIYANG DEPRESSION. Fractals, 2018, 26, 1840008.	1.8	19
78	A method for determining oil-bearing pore size distribution in shales: A case study from the Damintun Sag, China. Journal of Petroleum Science and Engineering, 2018, 166, 673-678.	2.1	19
79	The splicing of backscattered scanning electron microscopy method used on evaluation of microscopic pore characteristics in shale sample and compared with results from other methods. Journal of Petroleum Science and Engineering, 2018, 160, 207-218.	2.1	20
80	Inherent wettability of different rock surfaces at nanoscale: a theoretical study. Applied Surface Science, 2018, 434, 73-81.	3.1	51
81	Impacts of clay on pore structure, storage and percolation of tight sandstones from the Songliao Basin, China: Implications for genetic classification of tight sandstone reservoirs. Fuel, 2018, 211, 390-404.	3.4	98
82	Research on the characteristics of earthworm-like vibration drilling. Journal of Petroleum Science and Engineering, 2018, 160, 60-71.	2.1	9
83	Petrophysical characterization of oil-bearing shales by low-field nuclear magnetic resonance (NMR). Marine and Petroleum Geology, 2018, 89, 775-785.	1.5	137
84	Classification of microscopic pore-throats and the grading evaluation on shale oil reservoirs. Petroleum Exploration and Development, 2018, 45, 452-460.	3.0	78
85	Adsorbed and Free Oil in Lacustrine Nanoporous Shale: A Theoretical Model and a Case Study. Energy & Fuels, 2018, 32, 12247-12258.	2.5	41
86	Effect of Salinity on Source Rock Formation and Its Control on the Oil Content in Shales in the Hetaoyuan Formation from the Biyang Depression, Nanxiang Basin, Central China. Energy & Fuels, 2018, 32, 6698-6707.	2.5	42
87	Effect of Shale Lithofacies on Pore Structure of the Wufeng–Longmaxi Shale in Southeast Chongqing, China. Energy & Fuels, 2018, 32, 6603-6618.	2.5	34
88	Non-uniform subsidence and its control on the temporal-spatial evolution of the black shale of the Early Silurian Longmaxi Formation in the western Yangtze Block, South China. Marine and Petroleum Geology, 2018, 98, 881-889.	1.5	7
89	Shale gas reservoir characterization: A typical case in the Southeast Chongqing of Sichuan Basin, China. PLoS ONE, 2018, 13, e0199283.	1.1	13
90	Nuclear Magnetic Resonance <i>T</i> ₁ – <i>T</i> ₂ Map Division Method for Hydrogen-Bearing Components in Continental Shale. Energy & Fuels, 2018, 32, 9043-9054.	2.5	65

#	Article	lF	CITATIONS
91	Heterogeneity characterization of the lower Silurian Longmaxi marine shale in the Pengshui area, South China. International Journal of Coal Geology, 2018, 195, 250-266.	1.9	63
92	Permeability evaluation on oil-window shale based on hydraulic flow unit: A new approach. Advances in Geo-Energy Research, 2018, 2, 1-13.	3.1	19
93	Impact of coal ranks on dynamic gas flow: An experimental investigation. Fuel, 2017, 194, 17-26.	3.4	18
94	Keys to linking GCMC simulations and shale gas adsorption experiments. Fuel, 2017, 199, 14-21.	3.4	84
95	A three-dimensional high-resolution reservoir model of the Eocene Shahejie Formation in Bohai Bay Basin, integrating stratigraphic forward modeling and geostatistics. Marine and Petroleum Geology, 2017, 82, 362-370.	1.5	14
96	Pore characteristics of lacustrine mudstones from the Cretaceous Qingshankou Formation, Songliao Basin. Interpretation, 2017, 5, T373-T386.	0.5	9
97	Multi-component segmentation of X-ray computed tomography (CT) image using multi-Otsu thresholding algorithm and scanning electron microscopy. Energy Exploration and Exploitation, 2017, 35, 281-294.	1.1	27
98	Nanogeosciences: Research History, Current Status, and Development Trends. Journal of Nanoscience and Nanotechnology, 2017, 17, 5930-5965.	0.9	67
99	Type and Size Distribution of Nanoscale Pores in Tight Gas Sandstones: A Case Study on Lower Cretaceous Shahezi Formation in Songliao Basin of NE China. Journal of Nanoscience and Nanotechnology, 2017, 17, 6337-6346.	0.9	7
100	Nanopores and Adsorptivity Characteristics of Shale. Journal of Nanoscience and Nanotechnology, 2017, 17, 6452-6458.	0.9	0
101	Estimation of Enriched Shale Oil Resource Potential in E ₂ s ₄ ^L of Damintun Sag in Bohai Bay Basin, China. Energy & Fuels, 2017, 31, 3635-3642.	2.5	21
102	Combining rate-controlled porosimetry and NMR to probe full-range pore throat structures and their evolution features in tight sands: A case study in the Songliao Basin, China. Marine and Petroleum Geology, 2017, 83, 111-123.	1.5	69
103	Characterization of full pore size distribution and its significance to macroscopic physical parameters in tight glutenites. Journal of Natural Gas Science and Engineering, 2017, 38, 434-449.	2.1	41
104	Characterization of shale pore system: A case study of Paleogene Xin'gouzui Formation in the Jianghan basin, China. Marine and Petroleum Geology, 2017, 79, 321-334.	1.5	97
105	Evaluation of the Adsorbed Gas Amount in a Shale Reservoir Using the Three Compositions Adsorbing Methane (TCAM) Method: A Case from the Longmaxi Shale in Southeast Chongqing, China. Energy & Fuels, 2017, 31, 11523-11531.	2.5	11
106	Comprehensive polynomial simulation and prediction for Langmuir volume and Langmuir pressure of shale gas adsorption using multiple factors. Marine and Petroleum Geology, 2017, 88, 1004-1012.	1.5	18
107	Comparisons of SEM, Low-Field NMR, and Mercury Intrusion Capillary Pressure in Characterization of the Pore Size Distribution of Lacustrine Shale: A Case Study on the Dongying Depression, Bohai Bay Basin, China. Energy & Fuels, 2017, 31, 9232-9239.	2.5	63
108	Pore structure characteristics of tight sandstones in the northern Songliao Basin, China. Marine and Petroleum Geology, 2017, 88, 170-180.	1.5	92

#	Article	IF	CITATIONS
109	Gas generation characteristics of the lower cambrian niutitang shale in qiannan depression, China. Petroleum Science and Technology, 2017, 35, 1209-1216.	0.7	2
110	Classifying Multiscale Pores and Investigating Their Relationship with Porosity and Permeability in Tight Sandstone Gas Reservoirs. Energy & Fuels, 2017, 31, 9188-9200.	2.5	65
111	Quality grading system for tight sandstone reservoirs in the Quantou 4 Member, southern Songliao Basin, Northeast China. Interpretation, 2017, 5, T503-T522.	0.5	9
112	Reservoir spaces in tight sandstones: Classification, fractal characters, and heterogeneity. Journal of Natural Gas Science and Engineering, 2017, 46, 80-92.	2.1	61
113	Pore-scale characterization of tight sandstone in Yanchang Formation Ordos Basin China using micro-CT and SEM imaging from nm- to cm-scale. Fuel, 2017, 209, 254-264.	3.4	107
114	Effect of the Wettability on Two-Phase Flow Inside Porous Medium at Nanoscale: Lattice Boltzmann Simulations. Journal of Nanoscience and Nanotechnology, 2017, 17, 6620-6625.	0.9	1
115	Quantitative characterization on shale-hosted oil reservoir: A case study of argillaceous dolomite reservoir in the Jianghan Basin. Fuel, 2017, 206, 690-700.	3.4	33
116	A Method to Recover the Original Total Organic Carbon Content and Cracking Potential of Source Rocks Accurately Based on the Hydrocarbon Generation Kinetics Theory. Journal of Nanoscience and Nanotechnology, 2017, 17, 6169-6177.	0.9	4
117	Modeling of hydrocarbon adsorption on continental oil shale: A case study on n-alkane. Fuel, 2017, 206, 603-613.	3.4	63
118	Lower limits and grading evaluation criteria of tight oil source rocks of southern Songliao Basin, NE China. Petroleum Exploration and Development, 2017, 44, 505-512.	3.0	22
119	Surface Effect on Oil Transportation in Nanochannel: a Molecular Dynamics Study. Nanoscale Research Letters, 2017, 12, 413.	3.1	13
120	Study on CO2 huff-n-puff of horizontal wells in continental tight oil reservoirs. Fuel, 2017, 188, 140-154.	3.4	42
121	Lacustrine shale oil resource potential of Es 3 L Sub-Member of Bonan Sag, Bohai Bay Basin, Eastern China. Journal of Earth Science (Wuhan, China), 2017, 28, 996-1005.	1.1	13
122	Lacustrine Source Rock Deposition in Response to Coevolution of the Paleoenvironment and Formation Mechanism of Organic-Rich Shales in the Biyang Depression, Nanxiang Basin. Energy & Fuels, 2017, 31, 13519-13527.	2.5	29
123	A Precise Porosity Measurement Method for Oil-Bearing Micro/Nano Porous Shales Using Low-Field Nuclear Magnetic Resonance (LF-NMR). Journal of Nanoscience and Nanotechnology, 2017, 17, 6827-6835.	0.9	14
124	A Preliminary Study on the Nanometer Pores of Shahezi Dark Mudstones in the Xujiaweizi Fault Depression, Songliao Basin, NE China: Implications for Shale Gas Potential. Journal of Nanoscience and Nanotechnology, 2017, 17, 6957-6961.	0.9	1
125	Using Thickness of Adsorption Water Film to Determine Lower Limits of Physical Parameters of Unconventional Gas Reservoir—Taking Turpan-Hami Basin as an Example. Journal of Nanoscience and Nanotechnology, 2017, 17, 6262-6267.	0.9	3
126	Simulation and Thermodynamic Analysis of the Adsorption of Mixed CH ₄ and N ₂ on Silicalite-1 Molecular Sieve. Journal of Nanoscience and Nanotechnology, 2017, 17, 6732-6737.	0.9	1

#	Article	IF	CITATIONS
127	Adsorption Properties of Hydrocarbons (n-Decane, Methyl Cyclohexane and Toluene) on Clay Minerals: An Experimental Study. Energies, 2017, 10, 1586.	1.6	17
128	Research on the Mechanism of In-Plane Vibration on Friction Reduction. Materials, 2017, 10, 1015.	1.3	9
129	Type and Quantitative Evaluation of Micropores in Longmaxi Shale of Southeast Chongqing, China. Journal of Nanoscience and Nanotechnology, 2017, 17, 7035-7043.	0.9	2
130	Chemical and Isotopic Fractionation of Shale Gas During Adsorption and Desorption. Journal of Nanoscience and Nanotechnology, 2017, 17, 6395-6403.	0.9	5
131	Molecular Simulation of Oil Mixture Adsorption Character in Shale System. Journal of Nanoscience and Nanotechnology, 2017, 17, 6198-6209.	0.9	15
132	Nano to Micron-Sized Pore Types and Pore Size Distribution Revealed by Innovative Test Methods-Case Studies from Fluvial, Lacustrine and Marine Tight and Shale Oil and Gas Plays in China and U.S Journal of Nanoscience and Nanotechnology, 2017, 17, 6296-6306.	0.9	3
133	Microstructural Characterization of the Clay-Rich Oil Shales by Nuclear Magnetic Resonance (NMR). Journal of Nanoscience and Nanotechnology, 2017, 17, 7026-7034.	0.9	16
134	Characteristics and Origin of High Porosity in Nanoporous Sandy Conglomerates—A Case from Shahezi Formation of Xujiaweizi Fault Depression. Journal of Nanoscience and Nanotechnology, 2017, 17, 6139-6148.	0.9	3
135	Quantitative Characterization of the Effect of Interfacial Fluid Layer on Water Flow Inside Nano-Porous Medium Using the Lattice Boltzmann Method. Journal of Nanoscience and Nanotechnology, 2017, 17, 6216-6223.	0.9	1
136	Characterization of Nano to Micron-Scale Pore Structure in Tight Sand Gas Reservoir from Turpan-Hami Basin. Journal of Nanoscience and Nanotechnology, 2017, 17, 6096-6108.	0.9	3
137	Evolution of Micro/Nano Pore-Throat System and Its Storage Capacity in Tight Sandstones. Journal of Nanoscience and Nanotechnology, 2017, 17, 6738-6745.	0.9	0
138	Research of CO2 and N2 Adsorption Behavior in K-Illite Slit Pores by GCMC Method. Scientific Reports, 2016, 6, 37579.	1.6	31
139	Combining nuclear magnetic resonance and rate-controlled porosimetry to probe the pore-throat structure of tight sandstones. Petroleum Exploration and Development, 2016, 43, 1049-1059.	3.0	84
140	Microscopic pore structure in shale reservoir in the argillaceous dolomite from the Jianghan Basin. Fuel, 2016, 181, 1041-1049.	3.4	79
141	Organic porosity evaluation of Lower Cambrian Niutitang Shale in Qiannan Depression, China. Petroleum Science and Technology, 2016, 34, 1083-1090.	0.7	7
142	Comparison and integration of experimental methods to characterize the full-range pore features of tight gas sandstone—A case study in Songliao Basin of China. Journal of Natural Gas Science and Engineering, 2016, 34, 1412-1421.	2.1	95
143	The connectivity of reservoir sand bodies in the Liaoxi sag, Bohai Bay basin: Insights from three-dimensional stratigraphic forward modeling. Marine and Petroleum Geology, 2016, 77, 1081-1094.	1.5	25
144	Basin modelling of gas migration and accumulation in volcanic reservoirs in the Xujiaweizi Fault-depression, Songliao Basin. Arabian Journal of Geosciences, 2016, 9, 1.	0.6	3

#	Article	IF	CITATIONS
145	How to select an optimal surfactant molecule to speed up the oil-detachment from solid surface: A computational simulation. Chemical Engineering Science, 2016, 147, 47-53.	1.9	42
146	Classification and oil system of continental shale: Es3L sub-member of Bonan sag, Jiyang depression, Eastern China. Arabian Journal of Geosciences, 2016, 9, 1.	0.6	3
147	Extraction of kerogen from oil shale with supercritical carbon dioxide: Molecular dynamics simulations. Journal of Supercritical Fluids, 2016, 107, 499-506.	1.6	58
148	Quantitative Evaluation on the Elastic Property of Oil-Bearing Mudstone/Shale from a Chinese Continental Basin. Energy Exploration and Exploitation, 2015, 33, 851-868.	1.1	16
149	Molecular dynamics simulation of liquid alkane occurrence state in pores and slits of shale organic matter. Petroleum Exploration and Development, 2015, 42, 844-851.	3.0	67
150	Evaluation and Modeling of the CO ₂ Permeability Variation by Coupling Effective Pore Size Evolution in Anthracite Coal. Energy & Fuels, 2015, 29, 717-723.	2.5	16
151	Mechanism of oil molecules transportation in nano-sized shale channel: MD simulation. RSC Advances, 2015, 5, 25684-25692.	1.7	28
152	Shale oil occurring between salt intervals in the Dongpu Depression, Bohai Bay Basin, China. International Journal of Coal Geology, 2015, 152, 100-112.	1.9	82
153	Oil detachment from silica surface modified by carboxy groups in aqueous cetyltriethylammonium bromide solution. Applied Surface Science, 2015, 353, 1103-1111.	3.1	36
154	A new method for grading and assessing the potential of tight sand gas resources: A case study of the Lower Jurassic Shuixigou Group in the Turpan-Hami Basin, NW China. Petroleum Exploration and Development, 2015, 42, 66-73.	3.0	11
155	Key factors controlling the gas adsorption capacity of shale: A study based on parallel experiments. Applied Geochemistry, 2015, 58, 88-96.	1.4	73
156	Oil content in argillaceous dolomite from the Jianghan Basin, China: Application of new grading evaluation criteria to study shale oil potential. Fuel, 2015, 143, 424-429.	3.4	45
157	The formation environment and developmental models of argillaceous dolomite in the Xingouzui Formation, the Jianghan Basin. Marine and Petroleum Geology, 2015, 67, 692-700.	1.5	26
158	A comparison of experimental methods for describing shale pore features — A case study in the Bohai Bay Basin of eastern China. International Journal of Coal Geology, 2015, 152, 39-49.	1.9	155
159	Thermal effect of intrusive rock on hydrocarbon generation from organic matter. Arabian Journal of Geosciences, 2015, 8, 39-56.	0.6	4
160	Nanometer-Scale Pore Characteristics of Lacustrine Shale, Songliao Basin, NE China. PLoS ONE, 2015, 10, e0135252.	1.1	20
161	Palaeoenvironment and Its Control on the Formation of Miocene Marine Source Rocks in the Qiongdongnan Basin, Northern South China Sea. Scientific World Journal, The, 2014, 2014, 1-10.	0.8	3
162	Organoporosity Evaluation of Shale: A Case Study of the Lower Silurian Longmaxi Shale in Southeast Chongqing, China. Scientific World Journal, The, 2014, 2014, 1-9.	0.8	12

#	Article	IF	CITATIONS
163	Distribution, sources and health risk assessment of mercury in kindergarten dust. Atmospheric Environment, 2013, 73, 169-176.	1.9	51
164	3D thermal history modeling of the Xujiaweizi fault depression, Song Liao basin. , 2013, , .		0
165	Bulk Pyrolysis and Chemical Kinetic Characteristics of OM Related to the Occurrence of Immature-Low Mature Oils. Energy Exploration and Exploitation, 2012, 30, 71-88.	1.1	2
166	Classification and evaluation criteria of shale oil and gas resources: Discussion and application. Petroleum Exploration and Development, 2012, 39, 268-276.	3.0	184
167	Identification of the lower limit of high-quality source rocks and its relation to hydrocarbon accumulation—Taking the Beier Sag in the Hailaer Basin as an example. Petroleum Science, 2012, 9, 10-17.	2.4	10
168	Water Role and Its Influence on Hydrogen Isotopic Composition of Natural Gas during Gas Generation. Acta Geologica Sinica, 2011, 85, 1203-1210.	0.8	4
169	Hydrocarbon Generation Kinetic Characteristics from Different Types of Organic Matter. Acta Geologica Sinica, 2011, 85, 702-711.	0.8	8
170	Chemical kinetics study of hydrocarbon regeneration from organic matter in carbonate source rocks and its significance. Science in China Series D: Earth Sciences, 2007, 50, 536-543.	0.9	9
171	A generalised equivalent resistivity model in laminated and dispersed shaly sands. Exploration Geophysics, 2005, 36, 259-265.	0.5	0
172	Quantitative evaluation of coal as source rocks. Nonrenewable Resources, 1997, 6, 245-249.	0.1	0
173	Analysis of Main Controlling Factors of Natural CO2 Based on 3D Geological Modelling in the Northern Wuerxun Sag, Hailar Basin, China. Arabian Journal for Science and Engineering, 0, , 1.	1.7	0
174	The evaluation method of hydrocarbon yield of source rocks in open, semiopen, and closed systems: A case study on the K1qn Formation, northern Songliao Basin, China. Interpretation, 0, , 1-34.	0.5	0
175	Evolution of fractal pore structure in sedimentary rocks. Earth and Space Science, 0, , .	1.1	1